Simulation of a turbulent premixed open V-shaped flame using contour advection with surgery

B. H. Y. Tang* C. K. Chan* J. S. L. Lam†

(Received 25 October 2005, revised 24 June 2005)

Abstract

Despite its capability of high spatial resolution, simulation of turbulent flows with traditional Lagrangian (front tracking) scheme is often discouraged by numerical instability caused by clustering of marker nodes and topological changes of fronts. Contour advection surgery, being a robust front tracking scheme, limits the growth of front complexity during simulation without jeopardizing accuracy or efficiency. This is its advantage over traditional front-tracking schemes. Contour advection surgery, with incorporation of the reaction sheet model, can accurately simulate the propagation and advection of a turbulent premixed V-shaped flame. In this study, it is further tested with

*Department of Applied Mathematics, The Hong Kong Polytechnic University, Hung Hom, Hong Kong. mailto:blossom.hy.tang@polyu.edu.hk

†Environmental Protection Department, The Government of HKSAR, Hong Kong.

See http://anziamj.austms.org.au/V46/CTAC2004/Tang for this article, Published September 1, 2005. ISSN 1446-8735

ten values of vortex circulation. Upstream turbulence levels ranged over 1.8–19.8%. Results indicate that upstream turbulence increases the average flame length, flame zone area and the overall burning rate. Maximum values of estimated flame surface density Σ lie in the range 0.1–1.4/mm with all profiles displaying a skewness towards the burnt region. Similar to results from laboratory experiments, Σ values decrease with upstream turbulence. Contour advection surgery copes with intense turbulence. Better quantitative understanding of the scheme has also been acquired.

Contents

1 Introduction

Turbulent premixed combustion is widely used in a range of engineering devices and has attracted research interest over many years. Laboratory experiments are not always economical and numerical simulation is often employed to lessen the research and development costs. In the field of turbulent premixed combustion, of primary research interest is the accurate simulation of a premixed flame propagating in an ambient turbulent flow. Due to the nonlinear coupling of mechanical turbulence and combustion process, devising an accurate numerical method which is capable of capturing details of the propagation without masking the nature of physics, still remains a challenge today.

Consider a two-dimensional rod-anchored turbulent v-shaped premixed flame. This is one of the most common configurations employed for studying turbulent flame in laboratory experiments. Amongst the many theoretical models developed for simulating such flame numerically, the reaction sheet model [10] appears to be the most frequently invoked. This model allows the internal structure of the flame to be neglected because, when the reaction rate is high, the flame front can be approximated as an infinitesimally thin boundary separating burnt and unburnt regions. With the exclusion of the flame front's internal structure, the geometry of the flame front becomes the sole element that governs the evolution of the flow field. There are, in general, two approaches for capturing the flame front movement accurately. The first one is called the *front-capturing* approach which has been proved to be very successful in numerous works [1, 2, 13]. However, being Eulerian in nature, the spatial resolution is limited by the grid size of the computational domain. Thus any sub-grid features are not resolved by this grid-based approach. The second one, termed the *front-tracking* approach, being Lagrangian in nature, does not have such spatial resolution limitation. This approach has received some attention [11, 12]. However, in general applications, it remains less popular than the Eulerian approach. This is because it often encounters numerical instability when dealing with topological change of fronts and cusp

development, which are common occurrences in turbulent premixed flames. In order to exploit its advantage of high spatial resolution and thus capture of sub-grid features, this numerical instability problem must first be solved.

In view of this, Lam et al. [8] employed a front-tracking scheme known as Contour Advection with Surgery (CAS), based on a technique called contour surgery (CS) [5, 6], which was originally developed for geophysical research [16] to treat the topological changes of flame fronts and development of cusps. Results were compared with laboratory measurement [14] from which a remarkable resemblance was obtained. The present work is a continuation of the work done by Lam et al. [8] with the primary objective of acquiring a better quantitative understanding of this method. By varying the circulation of the vortices injected at the computational domain entrance, a wide range of upstream turbulence levels is obtained. Analysis is made on the resulting average flame length, flame area, flame surface density Σ and burning rate.

2 Basic equations

The main assumptions of the model are:

1. the reaction rate is high and consequently the flame front is considered to be infinitesimally thin;
2. burnt and unburnt regions have distinct uniform densities;
3. the Mach number is sufficiently small for the flow to be regarded as incompressible on either side of the flame;
4. the mechanism of vorticity production is inviscid.

At low Mach number, the velocity field u for the combustion process can be decomposed into three components, namely, u_s the solenoidal component

due to volume expansion across the flame front, u_r the rotational component due to vorticity distribution $\omega(x)$, and u_p the potential velocity field:

$$u = u_s + u_r + u_p \,, \tag{1}$$

The following threes equations describe the conditions which have to be satisfied by individual components

$$\nabla \cdot u_s = m\delta(x - x_{\text{flm}}) \,, \quad \nabla \times u_s = 0 \,, \tag{2}$$

where m is the volume source strength along the flame front, x is the position vector with subscript flm denoting the flame position and $\delta(\cdot)$ is the two-dimensional Dirac delta function:

$$\nabla \cdot u_r = 0 \,, \quad \nabla \times u_r = \omega(x) \,, \tag{3}$$

$$u_p = \nabla\phi \,, \tag{4}$$

where ϕ is the velocity potential of the incident flow.

It can be shown that

$$m = (\rho_u/\rho_b - 1)S_u \,, \tag{5}$$

where ρ_u and ρ_b are the densities of the unburnt and burnt regions respectively and S_u is the thermodiffusively stable laminar flame velocity which is, for weak curvature, approximated by

$$S_u = S_L(1 + \varepsilon\kappa) \,, \tag{6}$$

where ε is the Markstein length scale and κ is the local curvature which is taken as positive/negative when the centre of the circular arc lies left/right of the flame front.

In the present simulation, vorticity $\omega(x)$ has two sources. One source is the prescribed upstream turbulence and the flame front itself is another. The

vorticity generated from the latter source is also known as *flame-induced vorticity*. The upstream source is simulated by injecting small uniform circular vortices at the domain entrance. To account for the flame-induced vorticity, the flame front is divided into small segments of equal length Δs with one small uniform circular vortex introduced immediately behind the mid-point of each segment in each time step. The determination of this flame-induced vorticity involves the use of an expression proposed by Hayes [7] for the vorticity jump across the flame front:

$$[\omega] = \left(\frac{1}{\rho_b} - \frac{1}{\rho_u}\right) \nabla_t(\rho_u S_u) + \frac{\rho_b - \rho_u}{\rho_u S_u} \left\{ D u_t + u_t \nabla_t u_t - u_t u_n \kappa - u_n \nabla_t u_n \right\}, \tag{7}$$

where u_t and u_n respectively denote the relative tangential and absolute normal velocity components at the flame front, ∇_t represents the gradient along the flame front and D is the material time derivative taken at a point which always lies on the flame front and moves in a direction normal to the discontinuity as it moves. To simulate the diffusive effect of viscosity on vorticity distribution, both upstream turbulence and flame-induced vortices are treated with the Random Vortex Method [4].

3 Contour advection surgery

3.1 Front advection

With CAS, the flame front is discretized into an orderly set of connected marker nodes $\{x_i\}$. These are advected in every time step using the fourth-order Runge–Kutta scheme. In the present simulation, the V-flame front is oriented such that the unburnt/burnt region is always on the left/right side. To determine the curvature at one marker node x_i, the coordinates of two neighbouring marker nodes x_{i-1} and x_{i+1} are required. A circular arc is fitted

through the three marker nodes and the curvature

$$\kappa_i = \frac{2(a_{i-1}b_i - b_{i-1}a_i)}{|\mathbf{t}_i||\mathbf{e}_i|^2|\mathbf{e}_{i-1}|^2}\,, \tag{8}$$

where a and b denote the coordinate set of a marker node, $\mathbf{t}$ is the tangent vector at marker node x_i and $\mathbf{e}$ is the displacement vector. It can be deduced that when the centre of the circular arc lies to left/right of the front, a positive/negative curvature is obtained.

3.2 Contour surgery

A technique called contour surgery (CS) is employed to tackle the problem caused by topological changes or the clustering of marker nodes. After the flame front has propagated to a new position, the distance between nonadjacent marker nodes is calculated. When this distance is less than a prescribed threshold value δ (note that δ no longer denotes the delta Dirac function) a so-called surgery is performed. There are two types of surgery, namely *fission* and *fusion*. Fission/fusion is invoked when the two nonadjacent marker nodes with distance less than δ are on the same/different front(s). Essentially the fission surgery breaks a single front into two disconnected ones while the fusion surgery merges two disconnected fronts into one. Since the complexity of fronts is less than with CS, numerical errors caused by overshooting can be prevented.

3.3 Marker nodes redistribution

To overcome the numerical instability caused by clustering of marker nodes, it is necessary to carry out redistribution after surgery. Before redistributing, each front is divided into a number of segments demarcated by so called *corners*. A corner is a high curvature region when (x_{i-1},x_i) and (x_i,x_{i-1})

make an acute angle. Having located corners and segment demarcations, the average node density λ of each segments is

$$\lambda_i = \min\left(\frac{1}{\delta}, \frac{1}{2\mu}\left(\tilde{\tilde{\kappa}}_i + \frac{1}{L}\right)\right), \tag{9}$$

$$\tilde{\tilde{\kappa}}_i = \frac{\tilde{\tilde{\kappa}}_i + \tilde{\tilde{\kappa}}_{i+1}}{2}, \tag{10}$$

$$\tilde{\tilde{\kappa}}_i = \frac{(\tilde{\kappa}_{i-1}/|\mathbf{e}_{i-1}|) + (\tilde{\kappa}_i/|\mathbf{e}_i|)}{(1/|\mathbf{e}_{i-1}|) + (1/|\mathbf{e}_i|)}, \tag{11}$$

$$\tilde{\kappa}_i = \sqrt{\frac{1}{L^2} + \left(\frac{\kappa_i + \kappa_{i+1}}{2}\right)^2}, \tag{12}$$

where L is the characteristic length scale and $\mu \leq 1$ is a positive nondimensional input parameter for overall density of marker nodes. The redistribution of marker nodes for each segment depends on its calculated value of λ. Consecutive marker nodes are interpolated using piecewise cubic splines with continuous curvature κ_i at marker nodes in common.

4 Numerical experiments

We select parameters to match the experimental conditions used by Cheng [3] and the experimental set-up is shown in Figure 1. Parameters used are: inflow velocity $U_o = 5.5\,\mathrm{ms}^{-1}$, $S_L = 0.44\,\mathrm{ms}^{-1}$, $\rho_u/\rho_b = \tau = 6.7$ and $\varepsilon = 1\,\mathrm{mm}$. In this study a Reynolds number of 2.8×10^4 is obtained using U_o and the characteristic length taken as 50 mm (chosen to match the diameter of the inner core of the coaxial cylinder used in Cheng's experiments). The computational domain is 120 mm × 150 mm with a grid size of 1 mm. Upstream turbulence is incorporated by injecting 24 vortices at random along the domain entrance of $y = \pm 60\,\mathrm{mm}$. Care is taken to ensure that the same number of positive and negative vortices are introduced at each injection. The vortex radius is fixed at 1 mm throughout this study. Ten simulations are performed

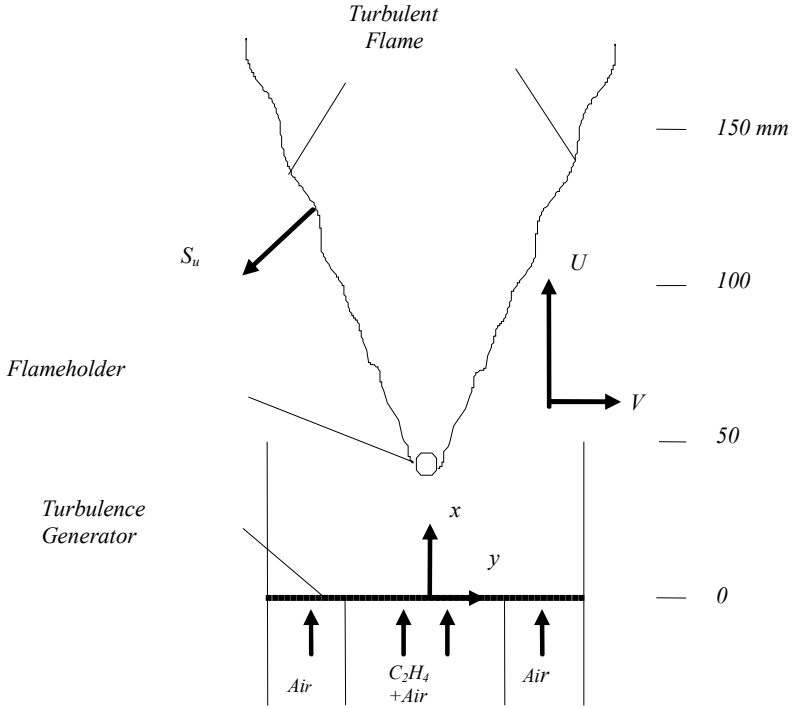

FIGURE 1: Experimental set-up for investigating a rod-stabilized V-shaped flame.

with the nondimensional vortex circulation starting at 0.002 and ascending in step of 0.002 to a vortex circulation of 0.02 . In all simulations, the nondimensional time step $\delta t = 0.005$. Vortices are introduced for every 10 time steps. A total of 5000 time steps are performed. All statistic results are obtained by averaging the instantaneous values after the 2000th time step.

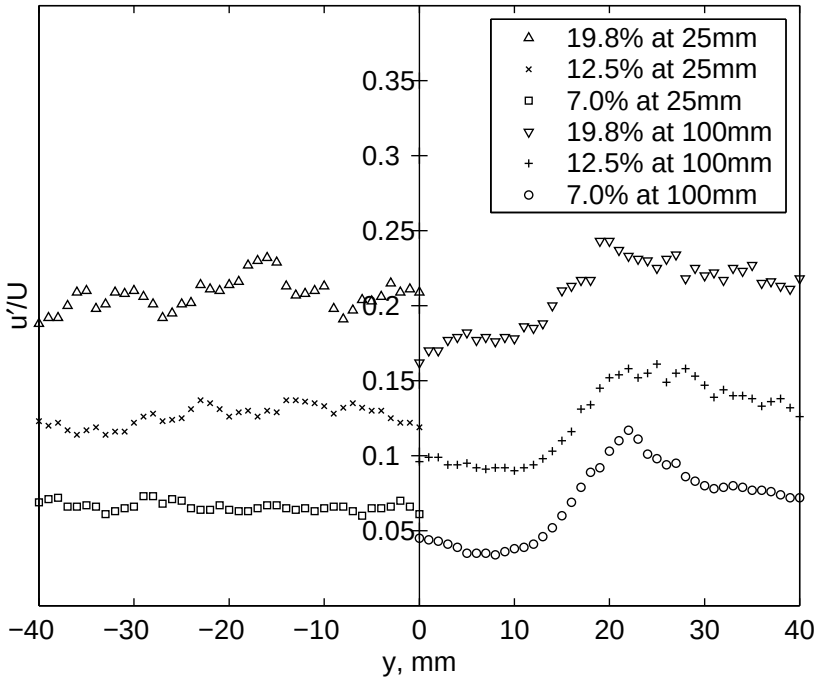

FIGURE 2: Upstream (left) and downstream (right) profiles of normalized velocity fluctuation u' of three selected cases.

4.1 Turbulence intensity

Resulted upstream mean turbulence intensities are 1.8%, 3.5%, 4.4%, 7.0%, 8.3%, 11.0%, 12.5%, 15.2%, 16.9% and 19.8%. Figure 2 shows profiles of RMS velocity fluctuation u' upstream ($x = 25\,\text{mm}$) and downstream ($x = 100\,\text{mm}$) of the flame holder which is located at $x = 50\,\text{mm}$. Profiles for three selected cases with turbulence levels of 7.0%, 12.5% and 19.8% (with vortex circulation of 0.008, 0.014 and 0.02 respectively) are presented. On the left hand side, profiles of upstream turbulence are shown. Clearly, upstream turbulence level increases with the circulation of injected vortices. Although the

circulation was raised linearly, the increase of upstream turbulence does not follow in the same fashion. On the right hand side, profiles of downstream turbulence are presented. All three profiles begin to display an obvious increase in turbulence intensity at $y = 10\,\text{mm}$. The profiles peak at a position just after $y = 20\,\text{mm}$. When the flow passes through the flame, density decreases rapidly while temperature increases across the flame resulting in local amplifications of velocity fluctuations. Hence, the peak on each profile represents the position of the flame front. From the figure, it can be deduced that the effect of increasing vortex circulation (hence turbulence intensity) on flame front position is negligible. It is also true that the peak (flame front position) is not as sharp at higher levels of turbulence intensities. This is because the extent of flame wrinkling is greater. Consequently, the flame has a thicker appearance and the corresponding peak becomes wider and less sharp.

Figure 3 shows the evolution of computed flame brush thickness along the axial direction. This is compared with values measured by Cheng [3]. Both sets of data are obtained under an upstream turbulence of 7.0%. See that the flame brush thickness has been slightly underestimated but the trend of an increasing flame brush thickness along the axial direction is captured successfully.

4.2 Flame surface density

In two dimensions, the flame surface density

$$\Sigma(\langle c\rangle) = \frac{\Delta L(\langle c\rangle)}{\Delta A(\langle c\rangle)}\,, \tag{13}$$

where $\Delta L\,(\langle c\rangle)$ and $\Delta A\,(\langle c\rangle)$ are respectively the average flame length and flame zone area. Both are expressed as a function of *mean reaction progress variable* $\langle c\rangle$ (hence the same applies to Σ). It depicts a fully burnt/unburnt region with a value of one/zero. Using the results from the three selected

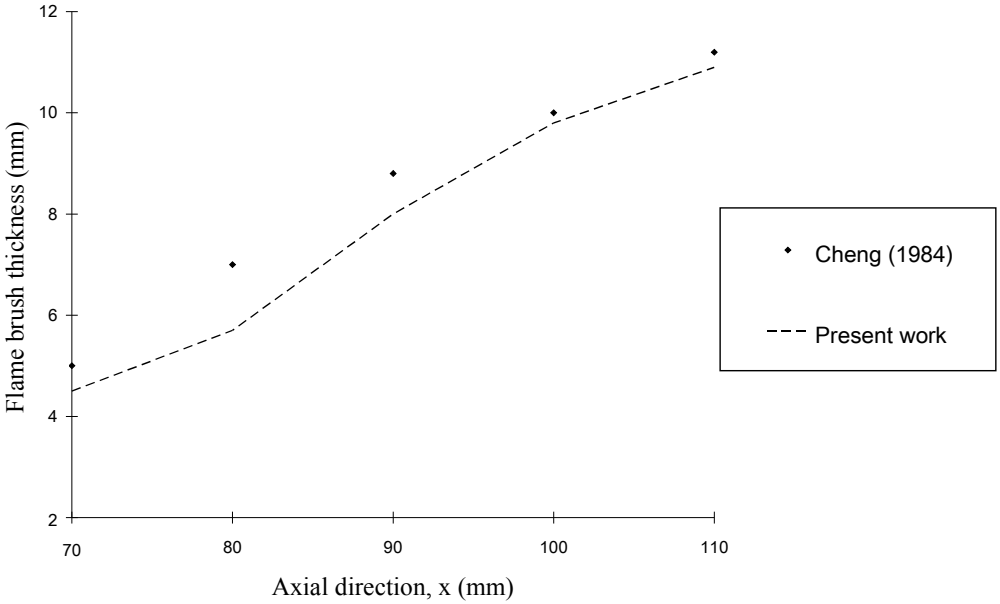

FIGURE 3: Comparison of computed and experimental flame brush thickness under an upstream turbulence of 7.0%.

simulations as before, Figure 4 is constructed to display the variations of ΔL and ΔA with $\langle c \rangle$. Figure 4 confirms that both ΔL and ΔA increase with turbulence. As mentioned in the preceding subsection, the extent of flame wrinkling is greater at higher level of turbulence. More wrinkling means longer flame length, thus explaining the trend observed in Figure 4. From individual subplots, the increase of ΔL with $\langle c \rangle$ becomes more apparent as turbulence intensity gets higher. Since there is greater cusping of the flame front on the burnt side, ΔL is longer at higher $\langle c \rangle$. Also, increased flame wrinkling causes the flame to thicken, which is displayed in Figure 4. All three ΔA profiles appear roughly symmetrical with a minimum at the centre of the flame zone ($\langle c \rangle = 0.5$). As anticipated, ΔA increases sharply as $\langle c \rangle$

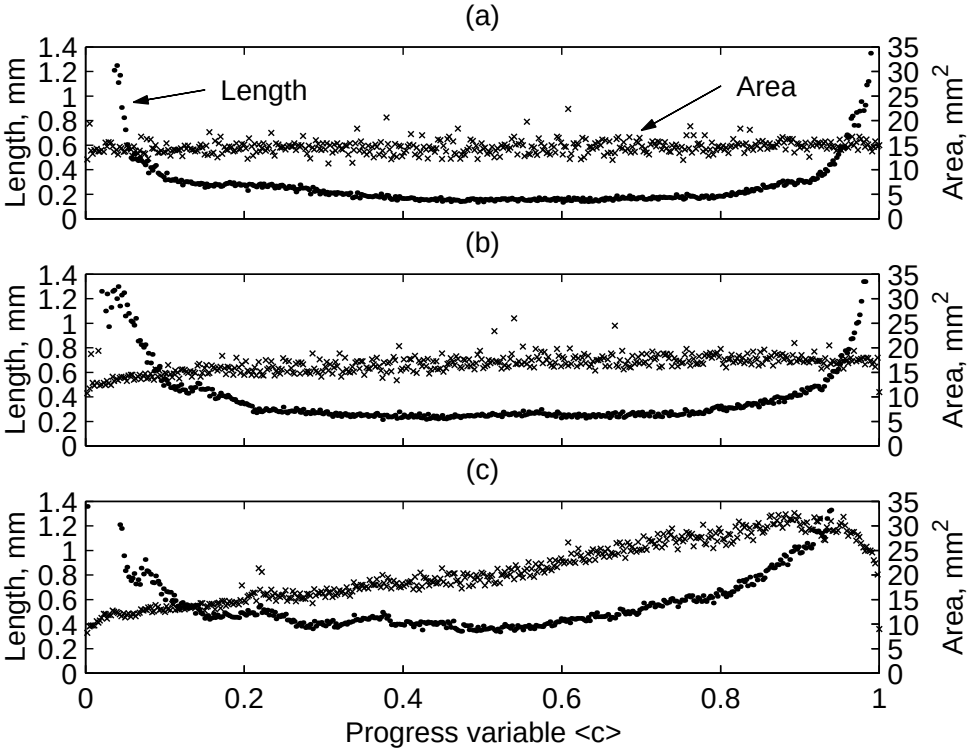

FIGURE 4: Variations of $\Delta L\,(\langle c\rangle)$ and $\Delta A\,(\langle c\rangle)$ with $\langle c\rangle$ for three different levels of upstream turbulence: (a) 7.0%, (b) 12.5%, (c) 19.8%.

tends to 0 (unburnt) and 1 (fully burnt).

Using values of ΔL and ΔA, the flame surface density Σ is estimated and results are illustrated in Figure 5. Asymmetry is observed for all profiles and are comparable in shape to those obtained by other researchers [14, 15] for a two-dimensional V-shaped flame, under different turbulence conditions. Skewing towards the burnt side is also observed. Results from some laboratory experiments [9] indicate that the peak of the profile moves further away from $\langle c\rangle = 0.5$ as turbulence increases. However, this is not apparent in the

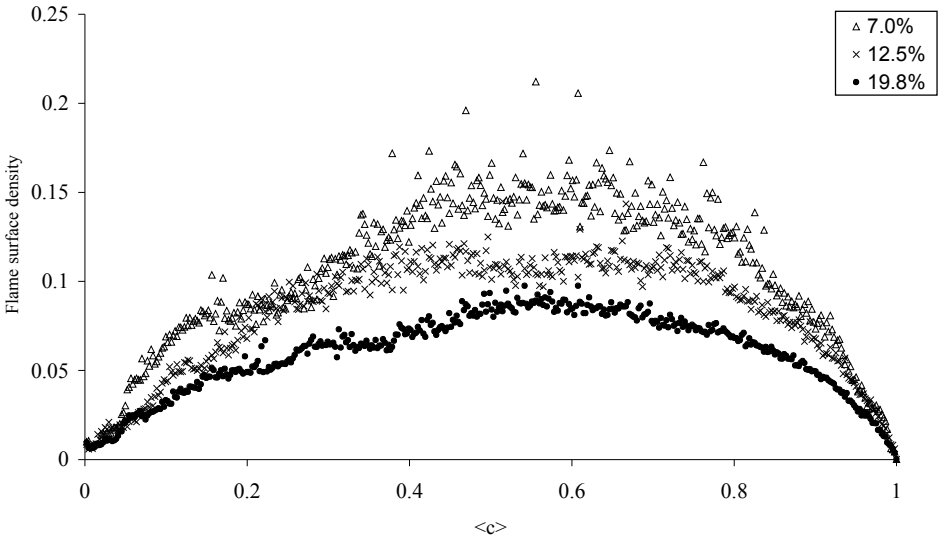

FIGURE 5: Variation of flame surface density with $\langle c \rangle$.

present simulations. Figure 6 compares the computed Σ profile with that measured by Shepherd [14] under a similar turbulence intensity. See that the profiles compare very well with similar maximum value and skewness towards the burnt side.

4.3 Overall burning rate

Following Shepherd [14], the estimated overall burning rate

$$W \approx \int_{\langle c \rangle = 0.05}^{\langle c \rangle = 0.95} \Sigma \, d\eta, \tag{14}$$

where η is an integration path which is normal to the $\langle c \rangle$ contours and takes a value of zero at $\langle c \rangle = 0.5$. Figure 5 illustrates that Σ is significantly less

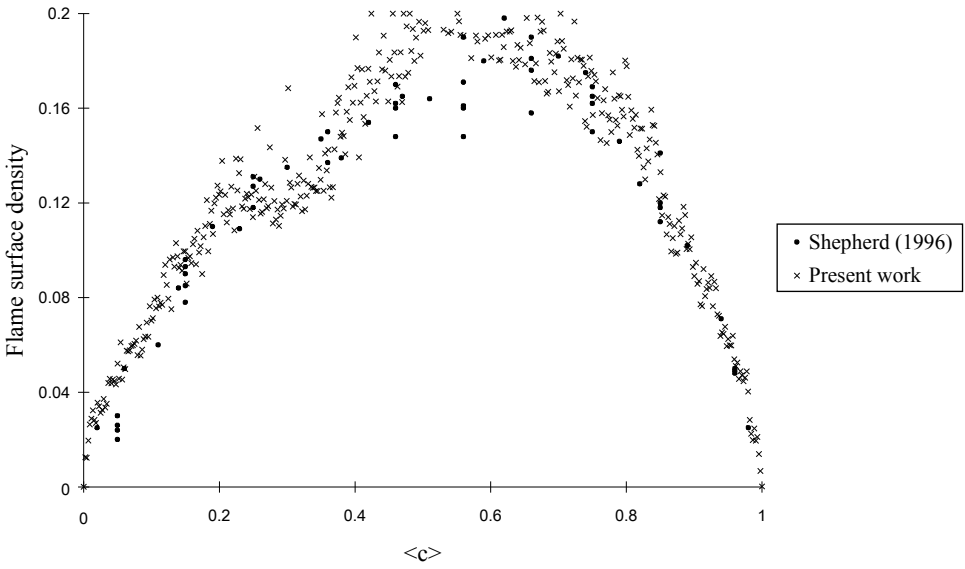

FIGURE 6: Comparison between computed and experimental flame surface density under an upstream turbulence of 7.0%.

at higher turbulence intensity. One might expect that lower Σ constitute lower W. However, the experimental data of Shepherd [14] illustrate that, W is *greater* at higher turbulence intensity. Hence a higher Σ does not necessary imply a higher W. As shown in Figure 4, the flame area increases with flame length. Since W is estimated by integrating Σ through the flame zone, it is possible for cases having low Σ but with higher W. The overall burning rates for all ten simulations are displayed in Figure 7. The minimum and maximum burning rates obtained are 1.26 and 3.36 respectively. Observe that the more intense the vortex circulation (and hence a higher upstream turbulence intensity), the greater the overall burning rate. A second order polynomial is fitted through the data points as an illustration that the rate of increase of W gets progressively higher with upstream turbulence. Using Figure 7 to estimate W for the V-shaped flame studied by Shepherd [14]

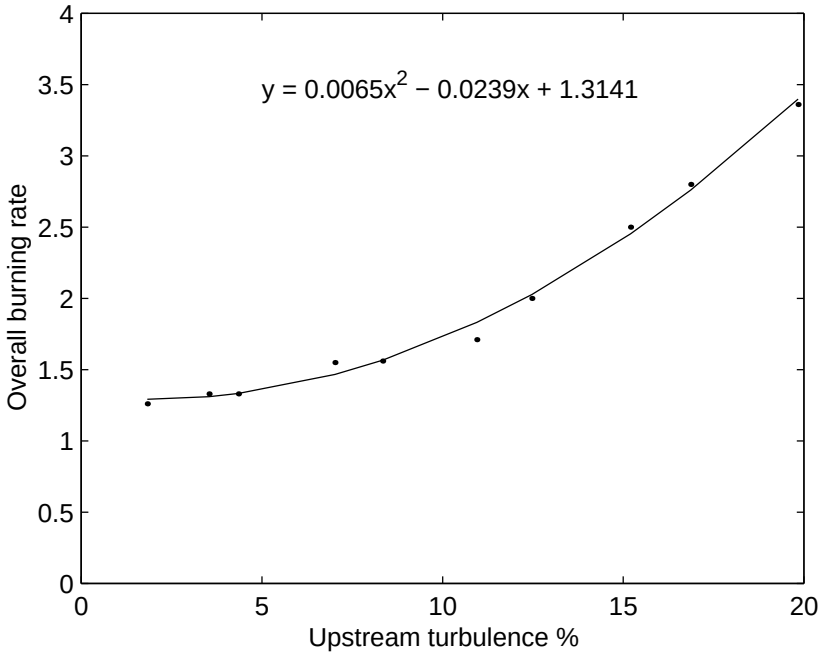

FIGURE 7: Variation of overall burning rate with upstream turbulence.

gives a value of 1.47, which is very close to the values shown in Table 2 of his paper.

5 Conclusions

Simulations tested a numerical algorithm termed Contour Advection with Surgery (CAS) applied to turbulent premixed combustion. Even at intense upstream turbulence, in excess of 15%, CAS can capture the flame front evolution with ease. Results confirm that both averaged flame length and flame zone area increase with turbulent intensity. Flame length is also longer in regions having higher values of mean progress variable $\langle c \rangle$. Profiles of the

flame surface density, Σ are comparable in shape to those obtained in similar laboratory experiments but as turbulence increases, the shifting of the peak away from $\langle c \rangle = 0.5$ is not observed. The minimum and maximum burning rate obtained are 1.26 and 3.36 respectively.

Acknowledgment: This work was partially supported by a studentship of The Hong Kong Polytechnic University and a grant from the Research Committed of The Hong Kong Polytechnic University (Grant No. A-PD99). We thank Mr. Hankel Fung for his help in using LaTeX.

References

[1] C. K. Chan, K. S. Lau and B. L. Zhang. Simulation of a premixed turbulent flame with the discrete vortex method. *Int. J. Numer. Meth. Eng.*, 48:613–627, 2000. C822

[2] C. K. Chan, H. Y. Wang and H. Y. Tang. Effect of intense turbulence on turbulent premixed V-flame. *Int. J. Eng. Sci.*, 41:903–916, 2003. C822

[3] R. K. Cheng. Conditioned sampling of turbulence intensities and Reynolds stress in premixed turbulent flame. *Combust. Sci. Technol.*, 41:109–142, 1984. C827, C830

[4] A. J. Chorin. Numerical study of slightly viscous flow. *J. Fluid Mech.*, 57:786–796, 1973. C825

[5] D. G. Dritschel. CS—a topological reconnection scheme for extended integrations using contour dynamics. *J. Comput. Phys.*, 77:240–266, 1988. C823

[6] D. G. Dritschel. Contour dynamics and CS: numerical algorithm for extended, high-resolution modelling of vortex dynamics in two-dimensional, inviscid, incompressible flows. *Comput. Phys. Rep.*, 10:78–146, 1989. C823

[7] H. D. Hayes. The vorticity jump across a gas dynamic discontinuity. *J. Fluid Mech.*, 2:595–600, 1959. C825

[8] J. S. L. Lam, C. K. Chan, L. Talbot and I. G. Shepherd. On the high-resolution modelling of a turbulent premixed open V-flame. *Combust. Theory Modelling*, 7:1–28, 2003. C823

[9] G. G. Lee, K. Y. Huh, and H. Kobayashi. Measurement and analysis of flame surface density for turbulent premixed combustion on a nozzle-type burner. *Combust. Flame*, 122:43–57, 2000. C832

[10] A. Linan and F. A. Williams. *Fundamental Aspects of Combustion.* Oxford University Press, 1993. C822

[11] M. Z. Pindera and L. Talbot. Some fluid dynamic considerations in the modeling of flames. *Combust. Flame*, 73:111–125, 1988. C822

[12] J. Qian, G. Tryggvason and C. K. Law. A front tracking method for the motion of premixed flames. *J. Comp. Phy.*, 144:52–69, 1998. C822

[13] C. W. Rhee, L. Talbot and J. A. Sethian. Dynamical behaviour of a premixed turbulent open V-flame. *J. Fluid Mech.*, 300:87–115, 1995. C822

[14] I. G. Shepherd. Flame surface density and burning rate in premixed turbulent flames. *Proc. Combust. Inst.*, 26:373–379, 1996. C823, C832, C833, C834

[15] D. Veynante, J. Piana, J. M. Duclos and C. Martel. Experimental analysis of flame surface density model for premixed turbulent combustion. *Proc. Combust. Inst.*, 26:413–420, 1996. C832

[16] D. W. Waugh and R. A. Plumb. Contour advection with surgery — a technique for investigating finescale structure in tracer transport. *J. Atmos. Sci.*, 51:530–540, 1994. C823